Editors' Suggestion | Featured in Physics

Electrically Controllable Kondo Correlation in Spin-Orbit-Coupled Quantum Point Contacts

Luke W. Smith,[1] Hong-Bin Chen,[1,2,3] Che-Wei Chang,[1] Chien-Wei Wu,[1] Shun-Tsung Lo,[1,4] Shih-Hsiang Chao,[1] I. Farrer,[5,6] H. E. Beere,[5] J. P. Griffiths,[5] G. A. C. Jones,[5] D. A. Ritchie,[5] Yueh-Nan Chen,[1,3] and Tse-Ming Chen[1,3,*]

[1]*Department of Physics, National Cheng Kung University, Tainan 701, Taiwan*
[2]*Department of Engineering Science, National Cheng Kung University, Tainan 701, Taiwan*
[3]*Center for Quantum Frontiers of Research and Technology (QFort), National Cheng Kung University, Tainan 701, Taiwan*
[4]*Department of Electrophysics, National Yang Ming Chiao Tung University, Hsinchu 300, Taiwan*
[5]*Cavendish Laboratory, University of Cambridge, Cambridge CB3 0HE, United Kingdom*
[6]*Department of Electronic and Electrical Engineering, University of Sheffield, Sheffield S1 3JD, United Kingdom*

(Received 15 June 2021; accepted 2 December 2021; published 10 January 2022)

Integrating the Kondo correlation and spin-orbit interactions, each of which have individually offered unprecedented means to manipulate electron spins, in a controllable way can open up new possibilities for spintronics. We demonstrate electrical control of the Kondo correlation by coupling the bound spin to leads with tunable Rashba spin-orbit interactions, realized in semiconductor quantum point contacts. We observe a transition from single to double peak zero-bias anomalies in nonequilibrium transport—the manifestation of the Kondo effect—indicating a controlled Kondo spin reversal using only spin-orbit interactions. Universal scaling of the Kondo conductance is demonstrated, implying that the spin-orbit interactions could enhance the Kondo temperature. A theoretical model based on quantum master equations is also developed to calculate the nonequilibrium quantum transport.

DOI: 10.1103/PhysRevLett.128.027701

The Kondo effect—which entails the many-body interaction between localized spins and their nearby itinerant electrons—is continuously of central interest in condensed matter physics. Not only is it a historical challenge with many still unresolved puzzles [1,2], but it also provides a powerful laboratory to study quantum spin correlations and coherence that could extend over micrometers [3], as well as to investigate other strongly correlated electronic systems [4,5]. One of the most intriguing problems among all Kondo systems is when it is associated with spin-unbalanced itinerant electrons. This has generally been realized by coupling the localized spin in a quantum dot to magnetic reservoirs, e.g., using ferromagnetic contacts and tuning the Kondo resonance through exchange-driven energy renormalization associated with quantum fluctuations [6–10]. This kind of system holds the key for controllable single-spin reversal as achieved by the use of ferromagnetic leads [8,9]. However, for greater impact in spin-related quantum technologies it is essential for the Kondo spin reversal to be controlled electrically.

Spin-orbit (SO) coupling—which links the electron spin to its motion—provides an ideal method of spin manipulation and has played a crucial role in both fundamental science and the advent of technologies. Intuitively, the combination of SO coupling and the Kondo correlation is a powerful paradigm for more comprehensive spin manipulation. However, thus far very few systems have been shown to harbor both effects, and most of them are in emergent materials [11–13]. The experimental demonstration and implementation of such interplay in a controllable nanostructure with single magnetic impurity is challenging. Prior experiments have been limited to measurements of multielectron quantum dots (QDs) with SO splitting of the energy levels [14,15] focusing on the role of the SO coupling in the QD energy spectrum, with the Kondo resonance merely a tool to probe the energy spectrum. In that case, the itinerant electrons are from the conventional spin-degenerate reservoirs in a well-established Kondo system. The inability to tune the SO coupling while retaining the electron number (and thus the unpaired electron spin) within the QD also creates difficulties for investigating their interplay and for realizing the Kondo spin reversal.

Here, we report on a system in which the Kondo correlation is coupled to and controlled by the leads with SO coupling. It is essential to study whether the SO coupling in the reservoirs can influence the Kondo correlation through exchange-driven energy renormalization, as previously achieved by the use of magnetic leads [6–10]. The study is accomplished using quantum point contacts (QPCs) with strong Rashba SO coupling, a one-dimensional (1D) constriction defined electrostatically in a two-dimensional electron gas of an InGaAs/InAlAs heterostructure [16], where the electric field leading to the Rashba SO coupling arises from the structural inversion asymmetry of the heterostructure [27,28]. QPCs are proven to be a powerful means for spin manipulation [29–31] and realization of the spin

transistor [30]. The Kondo effect can also occur in QPCs when conduction electrons interact with a quasibound spin that arises within a double-barrier potential of the QPC channel [32–35], which is shown schematically in Fig. 1(a). The microscopic origin of the quasibound state can be attributed to strong electron interactions associated with either Friedel oscillations [33,35] (a scenario recently also linked to the van Hove ridge [36]) or backscatterings induced by the potential barrier profile [34], although no consensus has yet been reached. Its interplay with SO coupling occurs regardless of its detailed microscopic origin. The Kondo effect manifests in QPCs as a zero-bias anomaly (ZBA), a peak in conductance centered around zero source-drain bias voltage ($V_{sd} = 0$). The peak splits as a function of in-plane magnetic field and is suppressed as T increases at a rate determined by the Kondo temperature T_K, similar to the manifestation of the Kondo effect in quantum dots. Prior to our work, most research in this context used systems with negligible SO coupling. One advantage of using QPCs over quantum dots is that the localized spin moment is strongly coupled to the neighboring electron reservoirs since the quasibound state within the QPC is shallow [33,34]; thus, the exchange-driven energy renormalization of the Kondo resonance is more pronounced. Figure 1(b) shows a simplified device schematic.

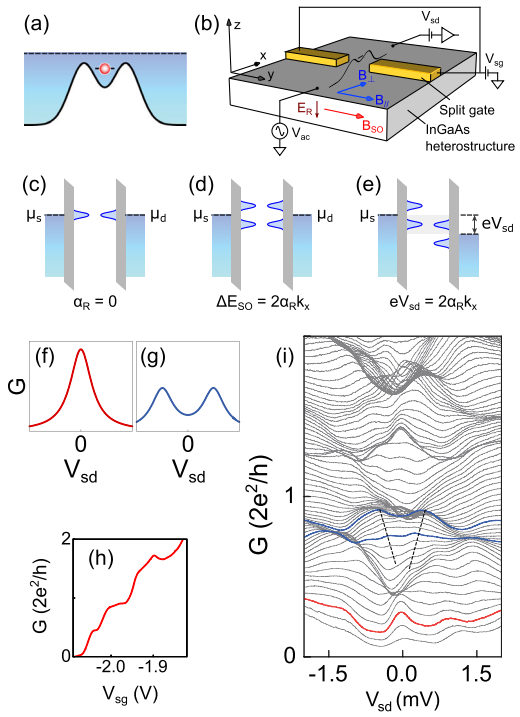

FIG. 1. Illustrations of the Kondo and spin-orbit-coupled system and zero-bias anomalies. (a) Schematic profile of the bound-state potential in the QPC. (b) Simplified circuit schematic. E_R and B_{SO} indicate directions of the electric field from the structural inversion asymmetry and the effective magnetic field due to SO coupling, respectively. (c)–(e) Energy-level diagrams of a Kondo impurity coupled to source and drain leads at three situations described in the text. (f),(g) Sketches of G against V_{sd} in the absence and presence of SO coupling, respectively. (h) QPC conductance at $V_{sd} = 0$. Plateaus are slightly suppressed below expected values due to imperfect transmission through the QPC. (i) QPC conductance as a function of V_{sd}, with V_{sg} stepped incrementally between traces.

Figures 1(c)–1(e) show schematic energy-level diagrams to illustrate the interplay between SO coupling and the Kondo effect. The Kondo resonance can be represented by a peak in the density of states (DOS) at the source and drain chemical potentials (μ_s and μ_d) arising from the interaction between an Anderson magnetic impurity and conduction electrons. Figure 1(c) represents the normal Kondo circumstance in which the localized spin is coupled to spin-degenerate leads, and the characteristic conductance enhancement, i.e., single-peak ZBA centered on $V_{sd} = 0$, is expected [Fig. 1(f)]. However, when the leads are spin unbalanced—e.g., by ferromagnetism [6–9], spin accumulation [10], or presumably the SO couplings as presented here—a spin splitting of Kondo resonances is expected even without any external magnetic field [Fig. 1(d)]. For a finite dc source-drain bias eV_{sd} equal to the spin splitting $\Delta E_{SO} = 2\alpha_R k_x$, where α_R parametrizes the strength of SO coupling and k_x is the electron wave vector, the local resonances in the source and drain DOS align as shown in Fig. 1(e) for the Kondo spin reversal to occur. This leads to a double-peak ZBA with peaks at $eV_{sd} = \pm 2\alpha_R k_x$ [Fig. 1(g)].

Figure 1(h) shows the differential conductance $G = dI/dV_{ac}$ for a QPC at $T = 22$ mK in the linear regime ($V_{sd} = 0$), where I is the source-drain current. In addition to standard conductance plateaus near integer multiples of $2e^2/h$ due to the 1D quantization of energy levels, a plateau is present roughly halfway between $G = 0$ and the first conductance plateau. Plateaus at $0.5 \times 2e^2/h$ have been observed in QPCs with strong SO coupling attributed to spin polarization driven by the SO coupling and electron-electron interactions [29], as has the conductance feature known as the 0.7 anomaly [37,38], which on some occasions is visible near $0.5 \times 2e^2/h$ when SO interactions are strong [39]. Figure 1(i) shows the nonlinear conductance G as a function of V_{sd} at different split-gate voltage V_{sg}. The classic single-peak ZBA, which is commonly observed in QPCs, occurs at certain V_{sg}, especially at low G when the 1D channel just opens, indicating relatively weak SO coupling in this regime. An example is highlighted in red. However, further from the pinch-off voltage when $G > \sim 0.5(2e^2/h)$, a double-peak ZBA emerges (the blue traces mark two examples). An increase of the peak splitting with G is observed for double-peak ZBAs and may be explained by a change in ΔE_{SO} due to α_R and k_F increasing with carrier density via the gate voltage, where previous measurements in an identical heterostructure show α_R increasing with density [30,31]. A qualitatively similar transition from the single-peak to double-peak ZBAs with

conductance has been observed in a GaAs QPC [35] but is attributed to the two-impurity Kondo effect since the SO coupling is negligibly small. Hence, deeper investigation into these double-peak ZBAs for our high SO material is essential to determine its origin.

The double-peak ZBA based on a scenario of the Kondo effect and SO coupling has a unique behavior in the influence of magnetic field. For the case where it is the time-reversal-symmetry breaking field (including ferromagnetism and spin accumulation) that leads to the spin splitting of Kondo resonances (and hence the splitting of ZBA), an external magnetic field will either enlarge or reduce the splitting depending on the orientation relative to the net polarization of the Kondo system. Although the SO interaction (which can also be viewed as an effective magnetic field B_{SO}), is also expected to lift the degeneracy and split the Kondo-enhanced conductance, a crucial difference is that B_{SO} and its resulting spin splittings are momentum dependent and, more importantly, time reversal symmetric. For external B parallel ($B_{\parallel}$) to B_{SO}, the spin splitting is simultaneously enlarged and reduced since B is parallel to B_{SO} for one momentum (k_F) but antiparallel to its opposite counterpart ($-k_F$). The two spin subbands of 1D leads are simply shifted vertically by the Zeeman energy. A distinctly different B dependence is predicted for B perpendicular ($B_{\perp}$) to B_{SO} since the two spin subbands become mixed and anticross [40,41]. The spin gap between these spin states in the eigenbasis is proportional to $\sqrt{B_{\perp}^2+B_{\mathrm{SO}}^2}$ and hardly varies in energy while $B_{\perp}<B_{\mathrm{SO}}$; therefore, the peaks should barely change with $B_{\perp}$.

Figures 2(a) and 2(b) show G as a function of V_{sd} at various $B_{\parallel}$ for the single- and double-peak ZBAs, respectively. In Fig. 2(a), the classic splitting of the Kondo-induced single-peak ZBA with increasing $B_{\parallel}$ is observed. The splitting is consistent with the magnetic-field dependence of the Kondo effect [32], i.e., $e\Delta V_{sd}\approx 2g^{*}\mu_B B_{\parallel}$, where ΔV_{sd} is the peak separation and Landé g factor $g^{*}=9$ for InGaAs [42]. For the double-peak ZBAs [Fig. 2(b)], the two peaks merge as $B_{\parallel}$ increases, forming a single peak around $B_{\parallel}\approx 1.4$ T, and continue to move past each other as $B_{\parallel}$ increases further. Their evolution is quantitatively consistent with a Zeeman splitting $2g^{*}\mu_B(B_{\parallel}-B_{\mathrm{SO}})$, with an offset B_{SO} accounting for the zero-field splitting. The same double-peak ZBA dependence with $B_{\parallel}$ for a second QPC is shown in the Supplemental Material [16].

Applying $B_{\perp}$ perpendicular to B_{SO} has a distinctly different effect. The single-peak ZBA [Fig. 2(c)] splits as $B_{\perp}$ increases with separation equal to twice the Zeeman energy, similar to $B_{\parallel}$. However, for the double-peak ZBA [Fig. 2(d)], the peak positions hardly change as $B_{\perp}$ increases from 0 to 0.8 T. The peaks remain at $V_{sd}\approx\pm 0.6$ mV, illustrated by the vertical lines, and have almost fully disappeared by $B_{\perp}=0.8$ T. The fact that the ZBAs survive to a much smaller $B_{\perp}$ than $B_{\parallel}$ may be due to the mixing and significant modification of the two spinful subbands driven by the interplay between the $B_{\perp}$ and SO interactions [40,41]. The SO effective magnetic field in Fig. 2(d) is estimated to be $B_{\mathrm{SO}}=1.15$ T using $e\Delta V_{sd}=2g^{*}\mu_B B_{\mathrm{SO}}$ assuming that the zero-field splitting is wholly attributed to SO coupling.

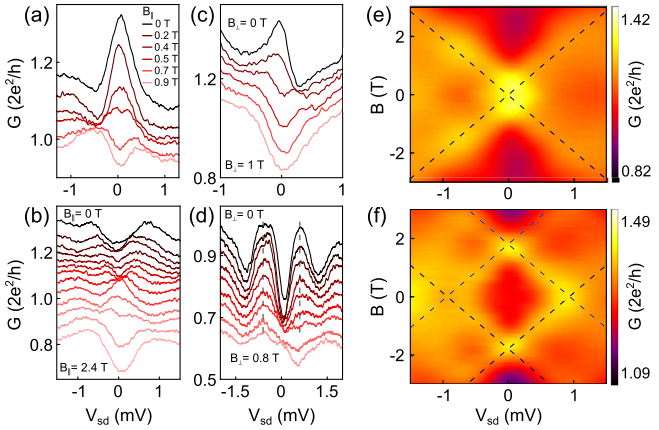

FIG. 2. Magnetic-field dependence of the single- and double-peak zero-bias anomalies. (a),(b) G as a function of V_{sd} for single- and double-peak ZBAs, respectively. The external magnetic field is applied parallel ($B_{\parallel}$) to B_{SO} and stepped between traces. (c),(d) Same as (a) and (b) but for the external magnetic field applied perpendicular ($B_{\perp}$) to B_{SO}. In (a)–(d) data are offset vertically for clarity. (e),(f) Color maps of G as a function of $B_{\parallel}$ and V_{sd} for the single- and double-peak ZBA, respectively. The positions of the ZBA peaks are well described by dashed lines $eV_{sd}=\pm g\mu_B(B_{\parallel}+B_{\mathrm{SO}})$ for (e) $B_{\mathrm{SO}}=0$ and (f) $B_{SO}=\pm 1.8$ T. B_{SO} in (f) differs from the estimate for Fig. 2(d) since data are measured at different V_{sg} and G. All data are obtained at $T=22$ mK.

Figures 2(e) and 2(f) show color maps of G as a function of $B_{\parallel}$ and V_{sd} for the case of a single-peak ZBA and a double-peak ZBA, respectively. Light (dark) colors indicate high (low) G, such that peaks in G correspond to bright diagonal regions. Dashed lines with a slope given by the Zeeman splitting of Kondo resonances are overlaid. Figure 2(e) shows the single-peak ZBA centered on $V_{sd}=0$ at $B_{\parallel}=0$ T splits at a rate of $eV_{sd}=\pm g\mu_B B_{\parallel}$ with $B_{\parallel}$ (marked with overlaid dashed lines), following the Zeeman splitting expected for Kondo resonances. For the double-peak ZBA [Fig. 2(f)], each of the two peaks split and dissolve into two crossing branches as $B_{\parallel}$ increases, although the outer pair of branches (i.e., at larger V_{sd}) are more blurred since the electrons are in a highly nonequilibrium transport region and may be heated by the large source-drain bias. These right and left moving branches follow the Zeeman splitting for SO-coupled Kondo resonance and represent energies $eV_{sd}=\pm g\mu_B(B_{\parallel}+B_{\mathrm{SO}})$, with the offset $g\mu_B B_{\mathrm{SO}}=2\alpha_R k_x$, which changes sign as the momentum reverses. The evolution of ZBA peaks is thus mirror symmetrical across both $B_{\parallel}$ and V_{sd}. The agreement

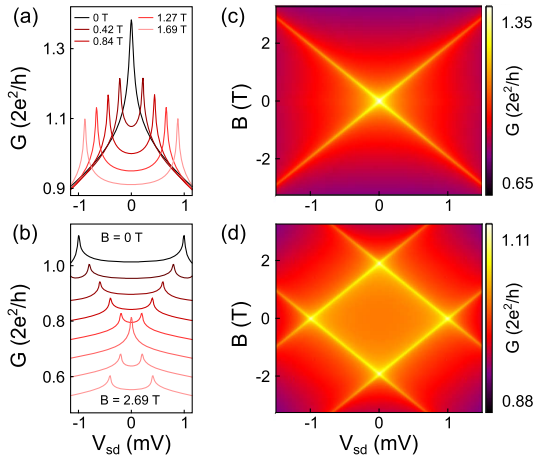

FIG. 3. Theoretical simulation of the differential conductance using a quantum master equation approach. (a),(b) G against V_{sd} in the absence and presence of Rashba SO coupling, respectively, for selected B. Data in (b) are offset vertically from $B = 0$ (top trace) in increments of $-0.06 \times 2e^2/h$ for clarity. Data in (a) are not offset. (c),(d) Corresponding color maps of G as a function of B and V_{sd} without and with SO coupling, respectively.

between the dashed lines and bright regions highlights the cohesiveness between the data and a scenario given by the Kondo effect with SO coupling. This is distinctly different from the double-peak ZBAs induced by a time-reversal-symmetry-broken spin imbalance and is also the opposite of that expected for the two-impurity Kondo system [35], in which the evolution with B depends mostly on the coupling between different impurities and reservoirs and the Zeeman energy is irrelevant.

We now present a theoretical basis for the nonequilibrium Kondo phenomenon with SO-coupled reservoirs and its behavior with magnetic field, with a full treatment given in the Supplemental Material [16]. Although the Landauer-Büttiker scattering theory and the nonequilibrium Green's function formalism are two standard approaches to capture the quantum nature of transport with the nonequilibrium Kondo effect, the application to some nontrivial cases becomes formidable. Attempts have therefore been made to develop a more convenient approach [43–45] based on quantum master equations (QMEs) in open systems [46,47]. However, this becomes cumbersome for cotunneling and Kondo problems which require higher-order expansions. An improved QME approach under the self-consistent Born approximation has been proposed [45] to efficiently account for higher-order tunneling contributions. This improved QME is capable of reproducing the Kondo peaks, but extending this approach to the Kondo problem with SO interactions is still challenging since the electron Fock state with a specific spin is no longer the eigenstate of the leads. Here, by introducing the *helicity* quantum number together with the orbital magnetic quantum number, we diagonalize the lead Hamiltonian in the presence of the Rashba SO term $\hat{H}_{\mathrm{SO}}$. Owing to the conservation of angular momentum, the problem can be effectively transformed into a two-channel Anderson model, where the effect of SO interactions is equivalent to coupling each spin state in the impurity to two helicities in the leads [16]. Figures 3(a) and 3(b) show G as a function of V_{sd} at selected values of $B_{\parallel}$ in the absence and presence of SO coupling, respectively. The corresponding color maps as a function of $B_{\parallel}$ are shown in Figs. 3(c) and 3(d), for the single- and double-peak ZBAs, respectively. The evolution of all the ZBA peaks follows the Zeeman term in good agreement with experimental observations.

The universal temperature dependence of G with T/T_K (i.e., the Kondo universal scaling) is a fundamental trait of the Kondo effect. This Kondo universality and its characteristic energy scale ($k_B T_K$) are crucial to identifying and understanding many-body correlations and quantum critical phenomena [1,48,49]. Figure 4(a) shows the T dependence of the single-peak ZBA at four different conductance values for $B = 0$ T. Peak heights at $V_{sd} = 0$ are plotted in Fig. 4(b) as a function of T. Solid curves show fits using the Anderson model for a Kondo impurity [50,51],

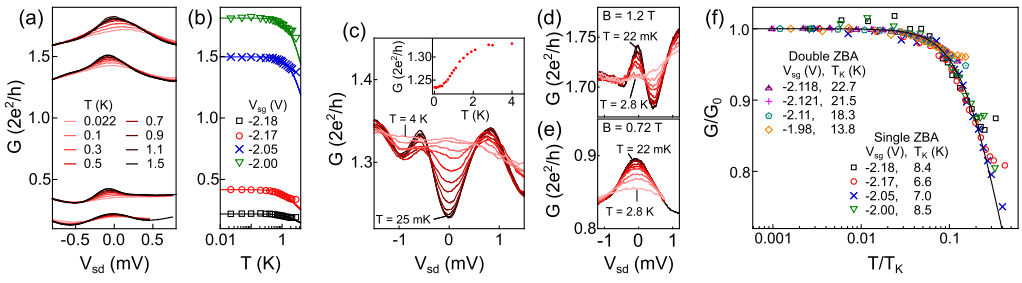

FIG. 4. Temperature dependence of single- and double-peak zero bias anomalies. (a) Temperature dependence of four different single-peak ZBAs ($B = 0$). (b) Peak height of ZBAs in (a) as a function of T measured at $V_{sd} = 0$. Solid lines are fits to the data using Eq. (1), with T_K as the fitting parameter. From top to bottom, $T_K = 8.5$, 7.0, 6.6, and 8.4 K. (c) Temperature dependence of the double-peak ZBA at $B = 0$. Inset: G against T at $V_{sd} = 0$. (d),(e) Temperature dependence of two double-peak ZBAs at $B_{\parallel} = 1.2$ and 0.72 T, respectively. The values of $B_{\parallel}$ are those where the peaks merge into a single peak. (f) Normalized ZBA peak height (G/G_0) at $V_{sd} = 0$ for both the single- and double-peak ZBAs. For each dataset G_0 is the ZBA peak height at base temperature and $V_{sd} = 0$. The black line is plotted using the Anderson model for a Kondo impurity [Eq. (1)].

$$G(T) = G_0[1 + (2^{1/s} - 1)(T/T_K)^2]^{-s}, \quad (1)$$

with T_K as the fitting (scaling) parameter, where G_0 is the zero-temperature conductance, and $s = 0.22$ for the spin-1/2 Kondo system. Above the first plateau, $2e^2/h$ is subtracted from G before fitting to remove the conductance from the first 1D subband. Similar values of T_K are obtained in all cases ($T_K = \sim$6–8 K). Deviations from Eq. (1) at high T are likely due to thermal fluctuations in the state occupancy.

Figure 4(c) shows the temperature dependence of the double-peak ZBA at $B = 0$ T. The peak heights decrease with T, while G between the peaks increases. The inset shows G at $V_{sd} = 0$ as a function of T. The conductance rises almost monotonically. This is opposite to a two-impurity Kondo system [35,52], where G is expected to decrease with T. We also plot the T dependence of several double-peak ZBAs with finite $B_\parallel$ applied, sufficient to merge the peaks, so they appear as a single peak. Figures 4(d) and 4(e) illustrate examples at two different V_{sg}, showing that the peak height reduces with T similar to Fig. 4(a). Figure 4(f) shows the Kondo universal scaling of G at $V_{sd} = 0$ for four such double-peak ZBAs with $B_\parallel$ applied, merging the peaks. The values of T_K estimated by fitting range from ~14 to 22 K, which is larger than the single peak. The single-peak data from Fig. 4(c) are also plotted for comparison.

There is a lack of consensus between theoretical works regarding how SO interactions influence the Kondo correlation, unaided by the lack of experimental data because of the challenge of realizing a Kondo system with a controllable SO interaction. Some theories predict exponential enhancement of T_K as SO interactions increase [53,54], whereas others suggest that it remains relatively unchanged [54,55]. Our estimates of T_K are larger when SO coupling appears to be significant (double-peak ZBAs present). Although it is difficult to draw definite conclusions from this limited dataset, the Kondo system presented here may suggest a new route to explore this fundamental spin correlation problem.

Integrating the Kondo effect and SO coupling in a single device and regulating their interactions may provide insight into many strongly correlated quantum systems associated with these two mechanisms, such as heavy fermion materials and topological Kondo materials. From a technological perspective, demonstrating electrical control of the spin degree of freedom removes any drawbacks associated with requiring external magnetic fields or ferromagnetic components, and thus could be significant for quantum-based technologies, including quantum computation and spintronics.

We thank M. Pepper for the helpful discussion. This work was supported by the Ministry of Science and Technology (Taiwan), the Higher Education Sprout Project, Ministry of Education to the Headquarters of University Advancement at the National Cheng Kung University (NCKU), the National Center for Theoretical Sciences (Taiwan), the U.S. Army Research Office (Grant No. W911NF-19-1-0081), and the Engineering and Physical Sciences Research Council (U.K.).

*tmchen@phys.ncku.edu.tw

[1] Z. Iftikhar, S. Jezouin, A. Anthore, U. Gennser, F. D. Parmentier, A. Cavanna, and F. Pierre, Two-channel Kondo effect and renormalization flow with macroscopic quantum charge states, Nature (London) **526**, 233 (2015).
[2] A. J. Keller, L. Peeters, C. P. Moca, I. Weymann, D. Mahalu, V. Umansky, G. Zaránd, and D. Goldhaber-Gordon, Universal Fermi liquid crossover and quantum criticality in a mesoscopic system, Nature (London) **526**, 237 (2015).
[3] I. V. Borzenets, J. Shim, J. C. H. Chen, A. Ludwig, A. D. Wieck, S. Tarucha, H.-S. Sim, and M. Yamamoto, Observation of the Kondo screening cloud, Nature (London) **579**, 210 (2020).
[4] A. C. Hewson, *The Kondo Problem to Heavy Fermions* (Cambridge University Press, Cambridge, England, 1993).
[5] Stefan Kirchner, Silke Paschen, Qiuyun Chen, Steffen Wirth, Donglai Feng, Joe D. Thompson, and Qimiao Si, Colloquium: Heavy-electron quantum criticality and single-particle spectroscopy, Rev. Mod. Phys. **92**, 011002 (2020).
[6] J. Martinek, J. Martinek, Y. Utsumi, H. Imamura, J. Barnaś, S. Maekawa, J. König, and G. Schön, Kondo Effect in Quantum Dots Coupled to Ferromagnetic Leads, Phys. Rev. Lett. **91**, 127203 (2003).
[7] A. N. Pasupathy, R. C. Bialczak, J. Martinek, J. E. Grose, L. A. K. Donev, P. L. McEuen, and D. C. Ralph, The Kondo effect in the presence of ferromagnetism, Science **306**, 86 (2004).
[8] J. R. Hauptmann, J. Paaske, and P. E. Lindelof, Electric-field-controlled spin reversal in a quantum dot with ferromagnetic contacts, Nat. Phys. **4**, 373 (2008).
[9] J. C. Oberg, M. R. Calvo, F. Delgado, M. Moro-Lagares, D. Serrate, J. Fernández-Rossier, and C. F. Hirjibehedin, Control of single-spin magnetic anisotropy by exchange coupling, Nat. Nanotechnol. **9**, 64 (2014).
[10] T. Kobayashi, S. Tsuruta, S. Sasaki, T. Fujisawa, Y. Tokura, and T. Akazaki, Kondo Effect in a Semiconductor Quantum Dot with a Spin-Accumulated Lead, Phys. Rev. Lett. **104**, 036804 (2010).
[11] M. Dzero, J. Xia, V. Galitski, and P. Coleman, Topological Kondo insulators, Annu. Rev. Condens. Matter Phys. **7**, 249 (2016).
[12] Y. Li, Q. Ma, S. X. Huang, and C. L. Chien, Thin films of topological Kondo insulator candidate SmB_6: Strong spin-orbit torque without exclusive surface conduction, Sci. Adv. **4**, eaap8294 (2018).
[13] J.-X. Yin *et al.*, Spin-orbit quantum impurity in a topological magnet, Nat. Commun. **11**, 4415 (2020).
[14] T. S. Jespersen, K. Grove-Rasmussen, J. Paaske, K. Muraki, T. Fujisawa, J. Nygård, and K. Flensberg, Gate-dependent spin-orbit coupling in multielectron carbon nanotubes, Nat. Phys. **7**, 348 (2011).

[15] Y. Kanai, R. S. Deacon, S. Takahashi, A. Oiwa, K. Yoshida, K. Shibata, K. Hirakawa, Y. Tokura, and S. Tarucha, Electrically tuned spin-orbit interaction in an InAs self-assembled quantum dot, Nat. Nanotechnol. **6**, 511 (2011).

[16] See Supplemental Material at http://link.aps.org/supplemental/10.1103/PhysRevLett.128.027701, which includes Refs. [17–26], for details on the materials and methods, measurements from a second QPC, and full details on the theoretical model.

[17] L. W. Smith *et al.*, Dependence of the 0.7 anomaly on the curvature of the potential barrier in quantum wires, Phys. Rev. B **91**, 235402 (2015).

[18] L. W. Smith *et al.*, Effect of Split Gate Size on the Electrostatic Potential and 0.7 Anomaly within Quantum Wires on a Modulation-Doped GaAs/AlGaAs Heterostructure, Phys. Rev. Applied **5**, 044015 (2016).

[19] S. Datta, *Electronic Transport in Mesoscopic Systems* (Cambridge University Press, New York, 1995).

[20] H. Haug and A.-P. Jauho, *Quantum Kinetics in Transport and Optics of Semiconductors*, 2nd ed. (Springer-Verlag, Berlin, 2007).

[21] S. Hershfield, J. H. Davies, and J. W. Wilkins, Probing the Kondo Resonance by Resonant Tunneling through an Anderson Impurity, Phys. Rev. Lett. **67**, 3720 (1991).

[22] J. Fransson, Nonequilibrium theory for a quantum dot with arbitrary on-site correlation strength coupled to leads, Phys. Rev. B **72**, 075314 (2005).

[23] M. Galperin, A. Nitzan, and M. A. Ratner, Inelastic transport in the Coulomb blockade regime within a nonequilibrium atomic limit, Phys. Rev. B **78**, 125320 (2008).

[24] H.-P. Breuer and F. Petruccione, *The Theory of Open Quantum Systems* (Oxford University Press, New York, 2002).

[25] J. Malecki, The two dimensional Kondo model with Rashba spin-orbit coupling, J. Stat. Phys. **129**, 741 (2007).

[26] X.-Q. Li, J. Luo, Y.-G. Yang, P. Cui, and Y. Yan, Quantum master-equation approach to quantum transport through mesoscopic systems, Phys. Rev. B **71**, 205304 (2005).

[27] J. Nitta, T. Akazaki, H. Takayanagi, and T. Enoki, Gate Control of Spin-Orbit Interaction in an Inverted $In_{0.53}Ga_{0.47}As/In_{0.52}Al_{0.48}As$ Heterostructure, Phys. Rev. Lett. **78**, 1335 (1997).

[28] T. Koga, J. Nitta, T. Akazaki, and H. Takayanagi, Rashba Spin-Orbit Coupling Probed by the Weak Antilocalization Analysis in InAlAs/InGaAs/InAlAs Quantum Wells as a Function of Quantum Well Asymmetry, Phys. Rev. Lett. **89**, 046801 (2002).

[29] P. Debray, S. M. S. Rahman, J. Wan, R. S. Newrock, M. Cahay, A. T. Ngo, S. E. Ulloa, S. T. Herbert, M. Muhammad, and M. Johnson, All-electric quantum point contact spin-polarizer, Nat. Nanotechnol. **4**, 759 (2009).

[30] P. Chuang *et al.*, All-electric all-semiconductor spin field-effect transistors, Nat. Nanotechnol. **10**, 35 (2015).

[31] S.-T. Lo *et al.*, Controlled spatial separation of spins and coherent dynamics in spin-orbit-coupled nanostructures, Nat. Commun. **8**, 15997 (2017).

[32] S. M. Cronenwett, H. J. Lynch, D. Goldhaber-Gordon, L. P. Kouwenhoven, C. M. Marcus, K. Hirose, N. S. Wingreen, and V. Umansky, Low-Temperature Fate of the 0.7 Structure in a Point Contact: A Kondo-like Correlated State in an Open System, Phys. Rev. Lett. **88**, 226805 (2002).

[33] T. Rejec and Y. Meir, Magnetic impurity formation in quantum point contacts, Nature (London) **442**, 900 (2006).

[34] F. Sfigakis, C. J. B. Ford, M. Pepper, M. Kataoka, D. A. Ritchie, and M. Y. Simmons, Kondo Effect from a Tunable Bound State within a Quantum Wire, Phys. Rev. Lett. **100**, 026807 (2008).

[35] M. J. Iqbal *et al.*, Odd and even Kondo effects from emergent localization in quantum point contacts, Nature (London) **501**, 79 (2013).

[36] D. H. Schimmel, B. Bruognolo, and J. von Delft, Spin Fluctuations in the 0.7 Anomaly in Quantum Point Contacts, Phys. Rev. Lett. **119**, 196401 (2017).

[37] K. J. Thomas, J. T. Nicholls, M. Y. Simmons, M. Pepper, D. R. Mace, and D. A. Ritchie, Possible Spin Polarization in a One-Dimensional Electron Gas, Phys. Rev. Lett. **77**, 135 (1996).

[38] A. P. Micolich, What lurks below the last plateau: Experimental studies of the $0.7 \times 2e^2/h$ conductance anomaly in one-dimensional systems, J. Phys. Condens. Matter **23**, 443201 (2011).

[39] K. L. Hudson *et al.*, New signatures of the spin gap in quantum point contacts, Nat. Commun. **12**, 5 (2021).

[40] Y. V. Pershin, J. A. Nesteroff, and V. Privman, Effect of spin-orbit interaction and in-plane magnetic field on the conductance of a quasi-one-dimensional system, Phys. Rev. B **69**, 121306(R) (2004).

[41] C. H. L. Quay, T. L. Hughes, J. A. Sulpizio, L. N. Pfeiffer, K. W. Baldwin, K. W. West, D. Goldhaber-Gordon, and R. de Picciotto, Observation of a one-dimensional spin-orbit gap in a quantum wire, Nat. Phys. **6**, 336 (2010).

[42] P. J. Simmonds, F. Sfigakis, H. E. Beere, D. A. Ritchie, M. Pepper, D. Anderson, and G. A. C. Jones, Quantum transport in $In_{0.75}Ga_{0.25}As$ quantum wires, Appl. Phys. Lett. **92**, 152108 (2008).

[43] S. Welack, M. Schreiber, and U. Kleinekathöfer, The influence of ultrafast laser pulses on electron transfer in molecular wires studied by a non-Markovian density-matrix approach, J. Chem. Phys. **124**, 044712 (2006).

[44] M. Esposito and M. Galperin, Transport in molecular states language: Generalized quantum master equation approach, Phys. Rev. B **79**, 205303 (2009).

[45] J. Jin, J. Li, Y. Liu, X.-Q. Li, and Y. Yan, Improved master equation approach to quantum transport: From Born to self-consistent Born approximation, J. Chem. Phys. **140**, 244111 (2014).

[46] H.-B. Chen, N. Lambert, Y.-C. Cheng, Y.-N. Chen, and F. Nori, Using non-Markovian measures to evaluate quantum master equations for photosynthesis, Sci. Rep. **5**, 12753 (2015).

[47] I. de Vega and D. Alonso, Dynamics of non-Markovian open quantum systems, Rev. Mod. Phys. **89**, 015001 (2017).

[48] H. E. Stanley, Scaling, universality, and renormalization: Three pillars of modern critical phenomena, Rev. Mod. Phys. **71**, S358 (1999).

[49] M. Grobis, I. G. Rau, R. M. Potok, H. Shtrikman, and D. Goldhaber-Gordon, Universal Scaling in Nonequilibrium Transport through a Single Channel Kondo Dot, Phys. Rev. Lett. **100**, 246601 (2008).

[50] T. A. Costi and A. C. Hewson, Transport coefficients of the Anderson model via the numerical renormalization group, J. Phys. Condens. Matter **6**, 2519 (1994).

[51] D. Goldhaber-Gordon, J. Göres, M. A. Kastner, H. Shtrikman, D. Mahalu, and U. Meirav, From the Kondo Regime to the Mixed-Valence Regime in a Single-Electron Transistor, Phys. Rev. Lett. **81**, 5225 (1998).

[52] R. Aguado and D. C. Langreth, Kondo effect in coupled quantum dots: A noncrossing approximation study, Phys. Rev. B **67**, 245307 (2003).

[53] M. Zarea, S. E. Ulloa, and N. Sandler, Enhancement of the Kondo Effect through Rashba Spin-Orbit Interactions, Phys. Rev. Lett. **108**, 046601 (2012).

[54] A. Wong, S. E. Ulloa, N. Sandler, and K. Ingersent, Influence of Rashba spin-orbit coupling on the Kondo effect, Phys. Rev. B **93**, 075148 (2016).

[55] R. Žitko and J. Bonča, Kondo effect in the presence of Rashba spin-orbit interaction, Phys. Rev. B **84**, 193411 (2011).